A promising fuel cell catalyst using non-precious metal oxide

Hamdy F M Mohamed[1,2*], E E Abdel-Hady[1], M F M Hmamm[2], M Ibrahim[1], H Ahmed[1], M Mondy[1]and H Yehia[1]

[1] Physics Department, Faculty of Science, Minia University, P.O. Box 61519 Minia, Egypt.
[2] Renewable Energy Science & Engineering Department, Faculty of Postgraduate Studies for Advanced Science (PSAS), Beni-Suef University, P.O. Box 62511 Beni-Suef, Egypt
* Corresponding author, e-mail: hamdyfm@gmail.com&hamdy.farghal@mu.edu.eg

Abstract. Fuel cell has two essential problems, its cost and the durability, which hinder its commercialization. Platinum is the ideal catalyst that has high activity, stability and selectivity but has high cost. An attempt has been done to find a cheaper catalyst instead of platinum. Zinc oxide nanoparticles were synthesized via sol-gel method using zinc acetate and citric acid in basic media with different calcination temperatures (420, 520 and 620 ^{o}C). From X-ray diffraction (XRD) patterns, the calculated particles size is 7.7, 15.6 and 19.3 nm as the calcination temperature of 420, 520 and 620^{o}C, respectively, indicating that the particles size increases with increasing the calcination temperature. Different concentrations (5 and 10 wt.%) of ZnO nanoparticles with 10 wt.% polyvinyl alcohol (PVA) were prepared and calcinated at 750 ^{o}C to get carbon/ZnO as a catalyst for fuel cell applications. A carbon core-shell surrounding by mono-disperse ZnO nanoparticles with large surface area that required for the new catalyst with believable morphology was shown by transmission electron microscope (TEM). Also, XRD presents high purity of the new composite with uniformly distinguishable peaks. Fourier transformation infrared (FTIR) spectroscopy shows the change in the carbon/ZnO nanoparticles spectra due to ZnO characteristic vibration band at 440-460 cm^{-1}. Cyclic voltammetry (CV) exhibits a good promising catalytic activity and current density with oxidation behaviour is reported. Finally, ZnO used to enhance carbon electrochemically performance as a result of a novel non-precious catalyst.

1. Introduction

Energy is a key element of the interaction between nature and society and affects the economic development as well as the future of human existence. Concerns associated with human health and environmental risks have arisen rapidly over the last decades. Many of these issues are related to the production, transformation and use of energy, for example acid rain, ozone depletion and global climate change. Scientists focus their efforts into developing energy production processes that will be beneficial towards a sustainable development and simultaneously will satisfy society's energy needs. Meeting the present needs without compromising the future should be achieved by using alternative sources of energy like the hydrodynamic, solar, wind, geothermal, etc. Development of new energy

system is necessary for sustaining growing economies, disengaged from oil. Fuel cells are one of the key future technologies similar to batteries with the exception of the continuous replenishment of the fuel. They promise to reduce the ecological impact by creating environmentally friendly by products while using renewable fuel sources. They can be employed in a variety of applications, due to their flexible power output and ranging from a few watts to megawatts. Understanding fuel cells are thus pertinent to the advancement and sustainability of our energy demanding lifestyles.

The key components of the polymer electrolyte membrane fuel cells (PEMFCs), as shown in Figure 1, are: (a) the anode that consists of a support, a diffusion layer and the catalyst where the oxidation reaction produces electrons that flow through the external load towards the cathode; (b) the electrolyte membrane whose aqueous pockets provide a path for the protons to diffuse and reach the cathode side; and (c) the cathode where the protons react with oxygen to produce water on the hosted catalyst/diffusion layer. Thus, the transport of reactants towards the reaction sites is crucial and can result in significant efficiencies [1]. In PEMFC, hydrogen (H_2) is fed continuously to the anode in which it oxidized and oxygen (O_2) reduced at cathode. Electrolyte membrane permits protons resulting from H_2 oxidation to pass to other side. As electrolyte membrane is electrically insulator so electrons released from broken H_2 bond could pass only through external circuit generating current. Water is produced as hydrogen ions recombine with reduced oxygen ions [2,3] as;

$$H_2 \rightarrow 2H^+ + 2e^- \quad (1)$$

$$\tfrac{1}{2}O_2 + 2H^+ + 2e^- \rightarrow H_2O \quad (2)$$

$$H_2 + \tfrac{1}{2}O_2 \rightarrow H_2O \quad (3)$$

Catalyst at both electrodes used for speeding oxidation and reduction process so there are different requirements should be existed for good performance catalyst as activity, selectivity, stability and poising resistance [4]. Platinum (Pt) is the best element that meets the requirements. The biggest barrier facing fuel cells to commercialize is the high price of Pt ratio that used. Considerable attentions for replacing Pt are made by alloying [5,6], layering [7,8], core-shell [9–16] and free Pt techniques. The use of transition-metal nanoparticles in catalysis is crucial as they mimic metal surface activation, selectivity and efficiency to heterogeneous catalysis [17,18]. Among transition-metal nanoparticles, ZnO has been of considerable interest because of the role of ZnO in solar cells, catalysts, antibacterial materials, gas sensors, luminescent materials, and photocatalyst [19]. Nano-ZnO, as heterogeneous catalyst, has received great attention because it is inexpensive, nontoxic catalyst. It has also environmental advantages, which is, minimum execution time, low corrosion, waste minimization, recycling of the catalyst, easy transport, and disposal of the catalyst. So, the aim of this work is to prepare and characterize ZnO nanoparticles with carbon support which work as a free Pt catalyst for fuel cell applications. Characterizations of the samples were done using x-ray diffraction (XRD), Fourier transformation infrared spectroscopy (FTIR), transmission electron microscopy (TEM) and cyclic voltammetry (CV).

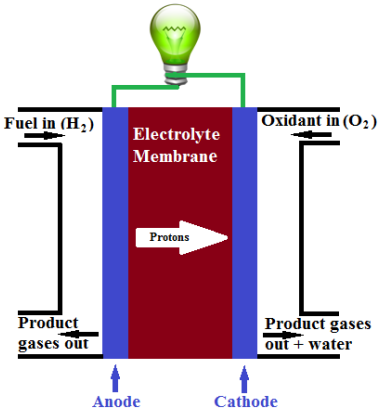

Figure 1. The polymer electrolyte membrane fuel cell (PEMFC).

2. Experimental setup

Zinc acetate dehydrate $Zn(O_2CCH_3)_2$ with purity more than 97% was purchased from Alfa Aeser, Germany, as a zinc source. A citric acid $C_6H_8O_7$ was purchased from Adwic, Egypt, and was used to react with the acetate to separate the zinc acetate to its parts. Zinc oxide nanoparticles were prepared using sol-gel method. This preparation is one of the simplest, environmental safe and lowest-cost technique for preparing pure transition metal oxides with relatively high surface area at low temperature. Adding ammonia solution was necessary for maintain the reaction pH at 8.5, prevent the solution from perception and get mono dispersal particles. Reagents and solvents were obtained from commercial sources and used without further purification. Three different samples were prepared at different calcination temperatures (420, 520 and 620 ^oC) with constant time (5h) as shown in Figure 2.

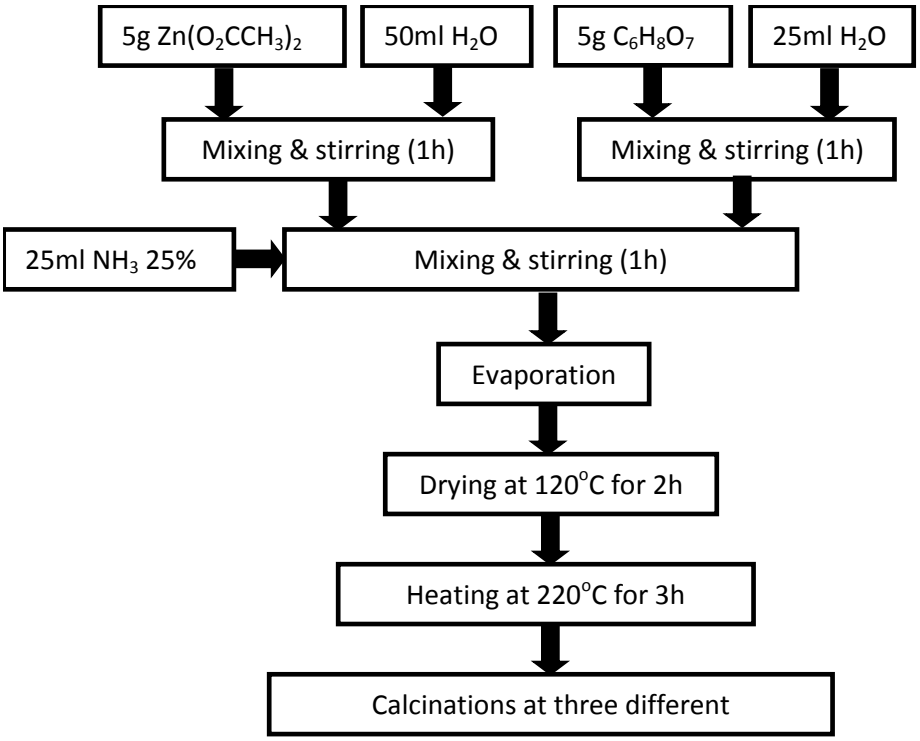

Figure 2. Synthesis of ZnO nanoparticles.

Polyvinyl alcohol (PVA) extra purity has purchased from Alpha Chemika with molecular weight 125000, which has low electrical conductivity, has been used as a carbon source. The mixture solution was prepared by dissolving PVA, 98-99% hydrolyzed in 20 ml of deionized water (10 wt.%). It was heated at 60 °C until the solution became clear (5–7h). Zinc oxide nanoparticles with two different concentrations (5 and 10 wt.%) were being dissolved in 5 ml of deionized water then added to the PVA solution and stirring the mixture for 24h until complete dissolving. Figure 3 shows the flowchart for the sample preparation.

X-ray diffraction (XRD) was measured for the present samples by Ultima IV (Rigaku Corporation) with a 285 mm goniometer. A parallel monochromatic x-ray beam acquired by reflection of CuKα radiation (λ = 1.542 Å) from a fine focus x-ray tube worked at 40 kV and 40 mA. Scattering profiles were recorded with a scintillation one-dimension position-sensitive detector over a range of $5^o < 2\theta < 70^o$ with a step of 0.01^o. The chemical structure of the samples under study turned into examined through FTIR using VERTEX 70 spectrometer, Bruker, USA, from wavenumber 4000 to 400 cm^{-1} with resolution 0.9 cm^{-1} at room temperature (25 ^oC).

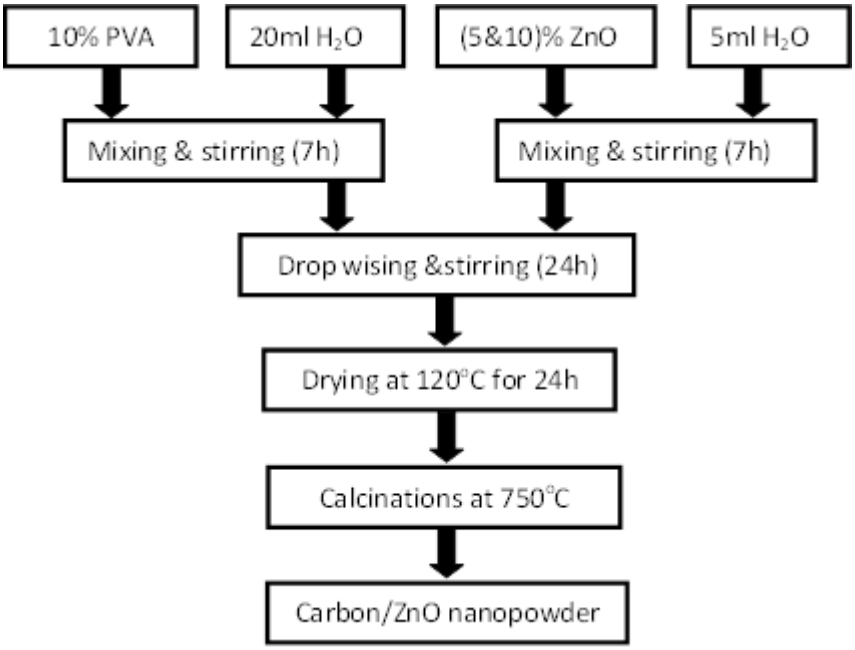

Figure 3. Synthesis of nanopowder of carbon/ZnO catalyst.

For electrochemical kinetic measurements, cyclic voltammetry (Autolab 302n potentiostat) at the National Research Center, Egypt, was used in the range of potential from -1 to -0.02 V with scan rates 50 and 100 mV/s and two different types of electrolytes (1M KOH and mixture of 1M KOH & 2M Methanol). Transmission electron microscopy (TEM) for carbon/ZnO nanoparticles 5 and 10 wt.% was carried out using JEOL JEM2100 made in USA for studying the surface and morphology. A few droplets of powder, ultrasonically dispersed in alcohol, had been put on standard microscope grid for the TEM work.

3. Results and Discussion

3.1. X-ray diffraction

X-ray diffraction (XRD) was used as crystal structure analysis for the three samples of ZnO nanoparticles calcinated at 420, 520, and 620 ^{o}C. Figure 4 illustrates the XRD pattern for the three different samples with very sharp peaks and narrow full width at half maximum (FWHM) which indicate the crystallinity in nature with clear diffraction peaks for wurtzite phase as mentioned in the standard data [19,20]. It is clear from the figure that, with increasing the calcination temperatures, the intensity of the peaks increases and also the FWHM decreases, that strongly suggesting good crystallinity of the nanomaterials. The peaks at 2θ = 31.67°, 34.31°, 36.14°, 47.40°, 56.52°, 62.73°, 66.28°, 67.91°, 69.03°, and 72.48° were assigned to (100), (002), (101), (102), (110), (103), (200), (112), (201), and (004), respectively of ZnO nanoparticles, indicating that the samples were polycrystalline wurtzite structure (Zincite, JCPDS 5-0664) [20–22]. For the three samples, no corresponding peaks for reactants remained were observed indicating that the prepared samples have a high purity. Sherrer's equation (equation (4)) could be used to determine the particle size as:

$$L_{hKL} = \frac{K\lambda}{B\cos(\theta)}. \quad (4)$$

Where L_{hkL} is the mean size of the particle, K is a dimensionless shape factor with a value close to unity, λ is the x-ray wavelength, β is the line broadening at the full width at half maximum (FWHM) in radians, and θ is the Bragg angle (in degrees). Table 1 lists the average particle size at different calcination temperatures for ZnO nanoparticles. It is clear from the table that, there is a correlation between varying the calcination temperature and the average particles size. Increasing in calcination temperature leads to increasing the grain size as the crystal structure rearranged, crystals agglomerate with each other, and removal of traces. Thus, in order to get smaller particles lower calcinations

temperature is favourable. By comparing the XRD pattern of the three samples it has been concluded that samples calcinated at 520 and 620 ^{o}C gives high intensity fine peaks, which can be used for further preparation and characterization.

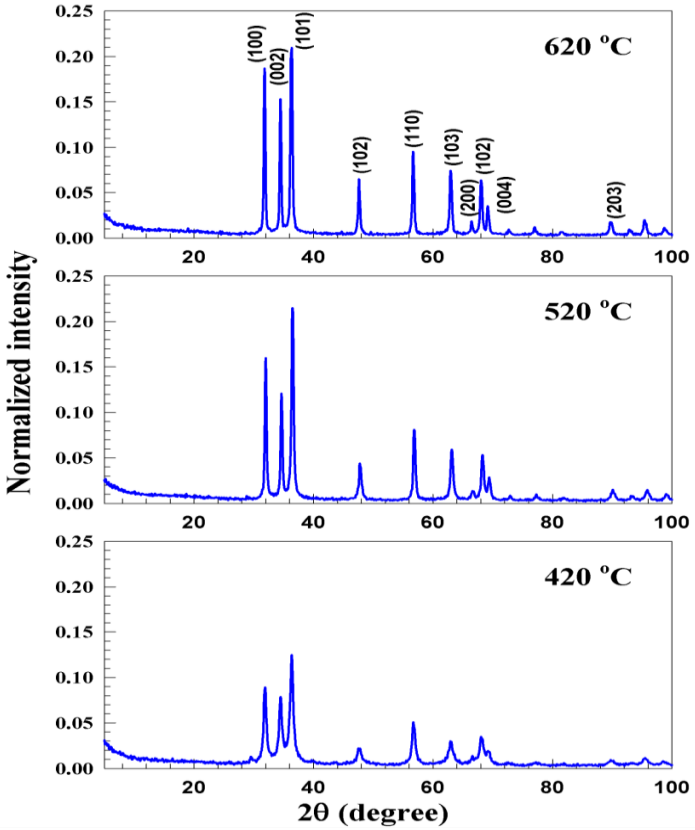

Figure 4. The XRD for the three ZnO nanoparticles calcinated at different temperatures.

The XRD for the two different concentrations of carbon/ZnO nanoparticles (5 and 10 wt.%) are similar and the high concentration is presented in Figure 5. It is noticed that, there is no significant difference between this XRD pattern and the other one in Figure 4 except the appearance of carbon hump at 2θ ~ 22^{o} similar to the data of Biswas *et al.* [23] and also decreasing the intensity of some peaks. This may be due to physical interaction between carbon and ZnO nanoparticles.

Table 1. Average particle sizes at different calcination temperature for ZnO nanoparticles.

Calcination temperature (^{o}C)	Average particles size (nm)
420	7.7
520	15.6
620	19.3

3.2. Fourier transformation infrared spectroscopy (FTIR)

FTIR used to study the catalyst's molecular structure as shown in Figure 6 for carbon/ZnO nanoparticles 5 and 10 wt.%. The figure shows a series of absorption peaks from 4000 to 400 cm^{-1}, which are corresponding to the carboxylate and hydroxyl impurities in the samples. For both samples, band at 3500 cm^{-1} is caused by stretching of hydroxyl group (O-H) and from 2700 to 3000 cm^{-1} band is corresponding to stretching vibration of C-H of alkane groups. The peaks at 1600 and 1100 cm^{-1} are

the results of stretching asymmetrically and symmetrically of the zinc carboxylate. Also, the characteristic bands at 459 and 445 cm^{-1} for carbon/ZnO nanoparticles of 5 and 10 wt.%, respectively, could be due to the vibration of the ZnO nanoparticles [24]. According to Verges [25], the single band centered at 460 cm^{-1} must be assigned to spherical particles, but when splitting occurs, prolative or platelike shapes are present. As the concentration of carbon (PVA) increases, the content of the carboxylate (COO^-) and hydroxyl (^-OH) groups in the samples decreased. The carboxylate probably comes from both of reactive carbon containing acetate species during synthesis and the hydroxyl results from the hygroscopic nature of ZnO. As a result, FTIR spectra suggest that some impurity exists near ZnO surface. This may be due to low calcination temperature and short time which they were not enough more to execute it as reported in the literature [26,27].

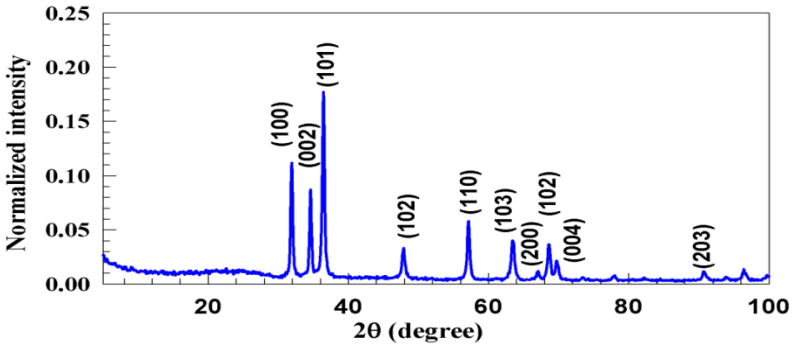

Figure 5. The XRD for carbon/ZnO (10 wt.%) nanoparticles.

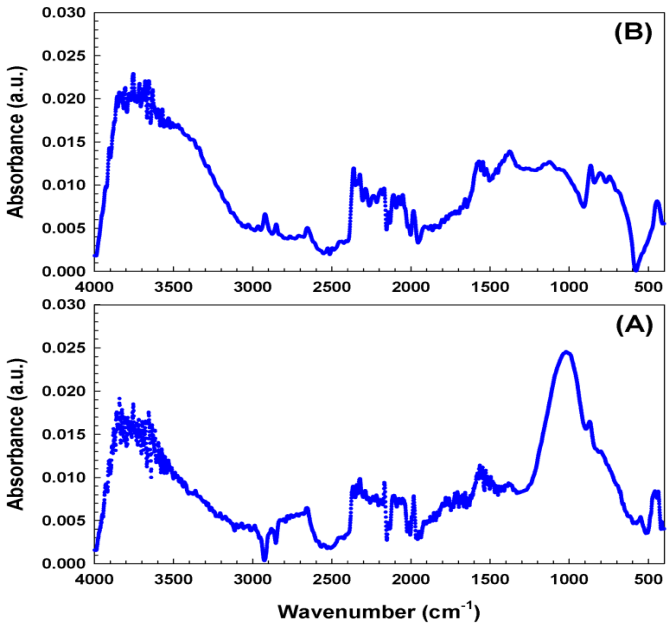

Figure 6. The FTIR spectra of carbon/ZnO nanoparticles (A) 5 wt.% and (B) 10 wt.%.

3.3. Transmission Electron Microscopy (TEM)

TEM images for the carbon/ZnO nanoparticles 5 and 10 wt.% are shown in Figure 7 and 8, respectively. From Figure 7, it is observed that there are nanoparticles of ZnO in the surface of the carbon with different morphology and randomly distribution. The ZnO nanoparticles are surrounding by carbon which provide more surface area. It well known that, larger active surface area is recommended for the catalyst requirements [28]. The average size of ZnO nanoparticles is 19.42 nm

which is in a good agreement with the XRD data [Table 1]. For high concentration of ZnO nanoparticles [Figure 8], the ZnO nanoparticles are widely distributed over a large range of carbon. In addition, the nanoparticles of ZnO had a better morphology (may be arranged as hexagonal crystals) than that in low concentration [Figure 7]. Also, there is a very good distribution of ZnO nanoparticles over a wide range of carbon compared to low concentration sample which support more surface area. Increasing the concentration of the ZnO nanoparticles affects the aggregations of nanoparticles over the carbon that make a core-shell of carbon surrounded by a high catalytic ZnO nanoparticles with large active surface area. From Figure 8, the average size of the carbon core-shell that surrounding by ZnO nanoparticles is found to be about 40 nm.

3.4. Cyclic voltammetry (CV)

Carbon/ZnO nanostructures (5 & 10 wt.%) were activated by applying cyclic voltages in 1M KOH and mixture of 1M KOH and 2M methanol electrolytes. The cyclic voltammetric behaviors of prepared samples are shown in Figure 9 with scan rate of 100 mV/s. Also, the cyclic voltammetric behaviors of standard Pt/C which is one of the most efficient commercial catalysts that has high activity is included. Carbon has low catalytic activity [29] that enhanced by adding ZnO nanoparticles with two different concentrations (5&10 wt.%). The electrocatalytic properties of carbon/ZnO powder were evaluated and compared with the commercial Pt/C. Table 2 lists the current density and applied voltage with 50 and 100 mV/s scan rate for the carbon/ZnO nanoparticles 5& 10 wt.% and also for Pt/C.

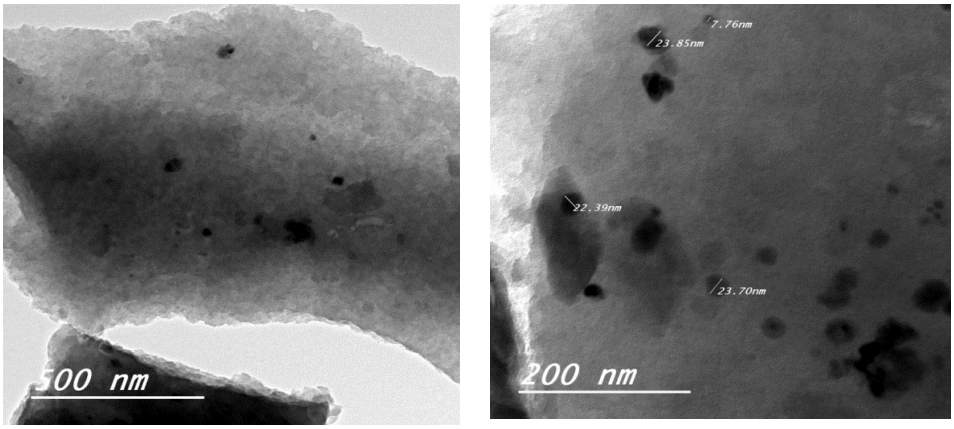

Figure 7. TEM images for the carbon/ZnO nanoparticles (5 wt.%) calcinated at 750 ^{o}C for 2h.

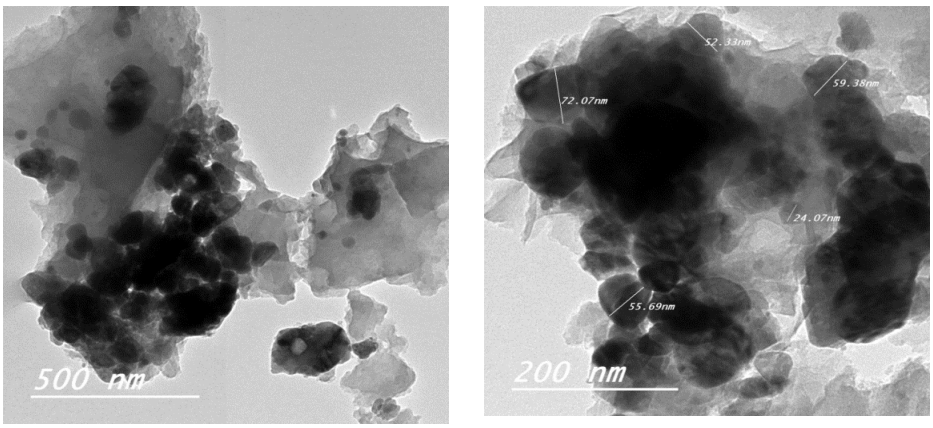

Figure 8. TEM images for the carbon/ZnO nanoparticles (10 wt.%) calcinated at 750 ^{o}C for 2h.

Carbon/ZnO 10 wt.% nanoparticles showed good oxidation behavior in KOH+methanol environment as the current density peak reaches 0.35 mA/cm^2 with scan rate 100 mV/s. On the other hand, the current density for carbon/ZnO (5 wt.%) was found to be 0.17 mA/cm^2. Increasing nanoparticles concentration increases the adsorption of OH in the electrolyte as more surface area was introduced for oxidation of methanol. Methanol oxidation peaks in anodic direction are reported with different intensities for carbon/ZnO nanoparticles (5&10 wt.%). Pt/C showed less current density in KOH reaches at maximum 0.55 mA/cm^2 while the highest current density of 5 wt.% sample is 0.06 mA/cm^2 at the same condition. For 10 wt.% sample, the oxidation peak height is almost three times as that in the 5 wt.% sample and nearly 33% of that for commercial Pt/C [Table 2]. Generally, it is understood that the anodic peak in the reverse scan to be linked to the removal of incompletely oxidized carbonaceous species accumulated on the catalyst surface during the forward anodic scan [30,31]. The oxidation peaks of KOH at anodic direction could be observed in all formulations. The obtained results of carbon/ZnO (10 wt.%) are comparative to commercial Pt/C activity which could be enhanced using carbon core-shell surrounded by more concentrations of ZnO nanoparticles with higher calcination temperatures.

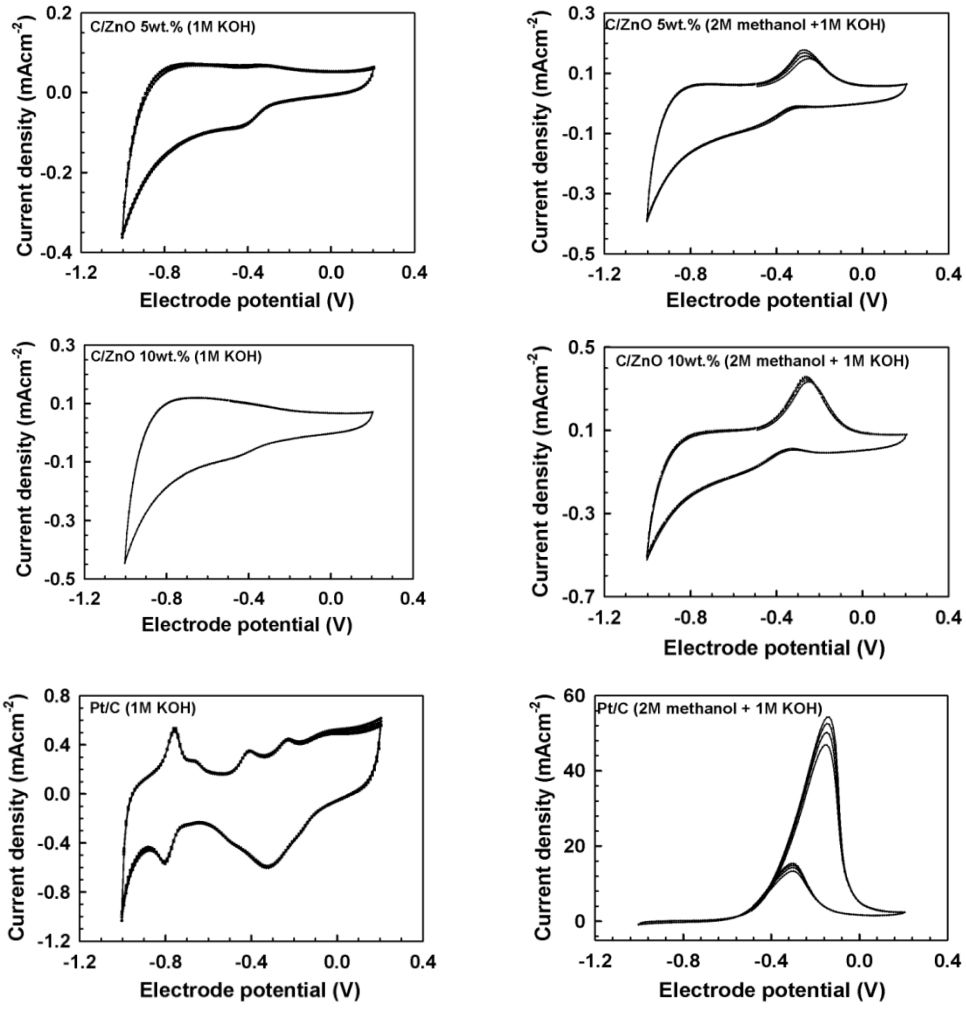

Figure 9. Consecutive CV of carbon/ZnO nanoparticles (5 & 10 wt.%) and Pt/carbon at scan rate of 100 mVs^{-1}.

Table 2. Current density and applied voltage for the carbon/ZnO nanoparticles 5 and 10 wt.% with different scan rates and different electrolyte. The data for Pt/C is also included for comparison.

Conditions/Samples		Pt/C		Carbon/ZnO (5 wt.%)		Carbon/ZnO (10 wt.%)	
Electrolyte	Scan rate (mV/s)	Current Density (mA/cm^2)	Applied voltage (V)	Current Density (mA/cm^2)	Applied voltage (V)	Current Density (mA/cm^2)	Applied voltage (V)
1M KOH	50	0.36	0.25	0.04	- 0.7	0.12	0.76
	100	0.55	0.28	0.06	- 0.75	0.14	0.76
2M Methanol +1M KOH	50	51	-0.2	0.14	-0.2	0.27	-0.25
	100	55	-0.2	0.17	-0.2	0.35	-0.28

4. Conclusion

ZnO nanoparticles with large surface area by sol-gel method were successfully synthesised with undertaken different calcination temperatures. XRD results for ZnO nanoparticles showed that the particles size increased directly with increasing calcination temperatures as the crystal structure rearranged, crystals agglomerated with each other, and traces were removed. The optimized temperature for preparing carbon/ZnO catalyst was 620 ^{o}C. According to XRD pattern and FTIR spectrum for the new catalyst, ZnO nanoparticles were adsorbed over carbon surface as physical interaction could be noticed. TEM images determined that carbon/ZnO has large surface area that is required for better catalytic activity. The core-shell of carbon surrounded by ZnO that successfully prepared provides high stability for the new catalyst. CV results proved that carbon active surface area and electrocatalytic performance enhanced by adding ZnO. Electrocatalytic properties of carbon increased in oxidation cycle by increasing the ZnO concentrations. The new catalyst using carbon support with different concentrations of ZnO nanoparticles improved the catalytic activity, thermal stability and surface corrosion for carbon. Carbon/ZnO was compared with commercial Pt/C and found that the sample of 10 wt. % efficiency reaches 33% of commercial Pt/C. Finally, carbon/ZnO catalyst after particular improvements can be used as a new generation of fuel cell operating by non-platinum catalyst.

Acknowledgement
The authors would like to thank the Academy of Scientific Research and Technology in Egypt (ASRT) for their financial support.

References

[1] O'Hayre R, Cha S W, Colella W and Prinz F B 2006 Fuel cell fundamentals
[2] Kordesch K S 1996 *Fuel cells and their applications* vol 117 (VCh Weinheim)
[3] Hoogers G, Chen E, Thompsett D, Hogarth M, Stone R and Hart D 2003 *Fuel Cell Technology Handbook* (CRC press)
[4] Holton O T and Stevenson J W 2013 The role of platinum in proton exchange membrane fuel cells *Platin. Met. Rev.* **57** 259–71
[5] Greeley J, Stephens I E L, Bondarenko A S, Johansson T P, Hansen H A, Jaramillo T F, Rossmeisl J, Chorkendorff I and Nørskov J K 2009 Alloys of platinum and early transition metals as oxygen reduction electrocatalysts *Nat. Chem.* **1** 552–6
[6] Stamenkovic V, Mun B S, Mayrhofer K J J, Ross P N, Markovic N M, Rossmeisl J, Greeley J and Nørskov J K 2006 Changing the Activity of Electrocatalysts for Oxygen Reduction by Tuning the Surface Electronic Structure *Angew. Chemie* **118** 2963–7
[7] Endoh E, Terazono S, Widjaja H and Takimoto Y 2004 Degradation Study of MEA for PEMFCs under Low Humidity Conditions *Electrochem. Solid-State Lett.* **7** A209
[8] Kinumoto T, Inaba M, Nakayama Y, Ogata K, Umebayashi R, Tasaka A, Iriyama Y, Abe T

and Ogumi Z 2006 Durability of perfluorinated ionomer membrane against hydrogen peroxide *J. Power Sources* **158** 1222–8
[9] Stephens I E L, Bondarenko A S, Perez-Alonso F J, Calle-Vallejo F, Bech L, Johansson T P, Jepsen A K, Frydendal R, Knudsen B P, Rossmeisl J and Chorkendorff I 2011 Tuning the Activity of Pt(111) for Oxygen Electroreduction by Subsurface Alloying *J. Am. Chem. Soc.* **133** 5485–91
[10] Zhao D and Xu B-Q 2006 Enhancement of Pt Utilization in Electrocatalysts by Using Gold Nanoparticles *Angew. Chemie Int. Ed.* **45** 4955–9
[11] Zhao D and Xu B-Q 2006 Platinum covering of gold nanoparticles for utilization enhancement of Pt in electrocatalysts *Phys. Chem. Chem. Phys.* **8** 5106–14
[12] Wang G, Huang B, Xiao L, Ren Z, Chen H, Wang D, Abruña H D, Lu J and Zhuang L 2014 Pt Skin on AuCu Intermetallic Substrate: A Strategy to Maximize Pt Utilization for Fuel Cells *J. Am. Chem. Soc.* **136** 9643–9
[13] Wang Y and Toshima N 1997 Preparation of Pd−Pt Bimetallic Colloids with Controllable Core/Shell Structures *J. Phys. Chem. B* **101** 5301–6
[14] Lim Y, Kim S K, Lee S-C, Choi J, Nahm K S, Yoo S J and Kim P 2014 One-step synthesis of carbon-supported Pd@Pt/C core–shell nanoparticles as oxygen reduction electrocatalysts and their enhanced activity and stability *Nanoscale* **6** 4038–42
[15] Zhou S, Varughese B, Eichhorn B, Jackson G and McIlwrath K 2005 Pt–Cu Core–Shell and Alloy Nanoparticles for Heterogeneous NOx Reduction: Anomalous Stability and Reactivity of a Core–Shell Nanostructure *Angew. Chemie Int. Ed.* **44** 4539–43
[16] Chen Y, Liang Z, Yang F, Liu Y and Chen S 2011 Ni–Pt Core–Shell Nanoparticles as Oxygen Reduction Electrocatalysts: Effect of Pt Shell Coverage *J. Phys. Chem. C* **115** 24073–9
[17] Durand J, Teuma E and Gómez M 2008 An Overview of Palladium Nanocatalysts: Surface and Molecular Reactivity *Eur. J. Inorg. Chem.* **2008** 3577–86
[18] Kung H H 1989 *Transition metal oxides: surface chemistry and catalysis* vol 45 (Elsevier)
[19] P N D and G 2010 ZnO nanoparticles and their applications-new achievements *Proceedings of the 2ndInternational Conference on Nanotechnology (NANOCON '10)* (Olomouc, Europe)
[20] Kulkarni S S, Sawarkar Mahavidyalaya S and Shirsat M D 2015 Optical and Structural Properties of Zinc Oxide Nanoparticles *Int. J. Adv. Res. Phys. Sci.* **2** 14–8
[21] Shalaby A, Bachvarova-Nedelcheva A, Iordanova R and Dimitriev Y 2013 A study of the effect of citric acid on the crystallinity of ZnO/TiO2 nanopowders *J. Chem. Technol. Metall.* **48** 585–90
[22] Bala N, Saha S, Chakraborty M, Maiti M, Das S, Basu R and Nandy P 2015 Green synthesis of zinc oxide nanoparticles using Hibiscus subdariffa leaf extract: effect of temperature on synthesis, anti-bacterial activity and anti-diabetic activity *RSC Adv.* **5** 4993–5003
[23] Biswas C, Bhattacharyya A, Chandra Das G, Choudhuri M G and Dey R 2016 A Novel Devolatilization Technique of Pre-reduction of Iron Ore Using Lean Grade Coal *BHM Berg- und Hüttenmännische Monatshefte* **161** 95–101
[24] Handore K, Bhavsar S, Horne A, Chhattise P, Mohite K, Ambekar J, Pande N and Chabukswar V 2014 Novel green route of synthesis of ZnO nanoparticles by using natural biodegradable polymer and its application as a catalyst for oxidation of aldehydes *J. Macromol. Sci. Part A* **51** 941–7
[25] Andrés-Vergés M and Martínez-Gallego M 1992 Spherical and rod-like zinc oxide microcrystals: morphological characterization and microstructural evolution with temperature *J. Mater. Sci.* **27** 3756–62
[26] Stoyanova A, Hitkova H, Bachvarova-Nedelcheva A, Iordanova R, Ivanova N and Sredkova M 2013 SYNTHESIS AND ANTIBACTERIAL ACTIVITY OF TiO 2 /ZnO NANOCOMPOSITES PREPARED VIA NONHYDROLYTIC ROUTE *J. Chem. Technol. Metall.* **48** 154–61
[27] Xiong G, Pal U, Serrano J G, Ucer K B and Williams R T 2006 Photoluminesence and FTIR study of ZnO nanoparticles: the impurity and defect perspective *Phys. Status Solidi* **3** 3577–81
[28] Dirote E V 2006 *Nanotechnology at the Leading Edge* (Nova Publishers)

[29] Trimble S W 2007 *Encyclopedia of Water Science, Second Edition - Two Volume Set (Print Version)* (CRC press)
[30] Sun S, Zhang G, Gauquelin N, Chen N, Zhou J, Yang S, Chen W, Meng X, Geng D and Banis M N 2013 Single-atom catalysis using Pt/graphene achieved through atomic layer deposition *Sci. Rep.* **3** 1775
[31] Mancharan R and Goodenough J B 1992 Methanol oxidation in acid on ordered NiTi *J. Mater. Chem.* **2** 875–87